HVAC&R Research

ISSN: 1078-9669 (Print) 1938-5587 (Online) Journal homepage: http://www.tandfonline.com/loi/uhvc20

A Methodology for Diagnosing Multiple Simultaneous Faults in Vapor-Compression Air Conditioners

Haorong Li & James E. Braun

To cite this article: Haorong Li & James E. Braun (2007) A Methodology for Diagnosing Multiple Simultaneous Faults in Vapor-Compression Air Conditioners, HVAC&R Research, 13:2, 369-395

To link to this article: https://doi.org/10.1080/10789669.2007.10390959

Published online: 25 Feb 2011.

A Methodology for Diagnosing Multiple Simultaneous Faults in Vapor-Compression Air Conditioners

Haorong Li, PhD
Member ASHRAE

James E. Braun, PhD, PE
Fellow ASHRAE

Received October 6, 2005; accepted September 5, 2006

Existing methods addressing automated fault detection and diagnosis (FDD) for vapor-compression air-conditioning equipment have good performance for faults that occur individually but have difficulty handling multiple simultaneous faults. In addition, these methods either require high-cost measurements or measurements over a wide range of conditions for training reference models, the development of which can be time consuming and cost prohibitive. This paper formulates model-based FDD in a generic way and demonstrates that decoupling is the key to handling multiple simultaneous faults. To eliminate a cost-prohibitive overall system model, an alternative physical decoupling methodology to mathematical decoupling is developed. During the mathematical development, a previously developed FDD method termed the statistical rule-based method *is reexamined and cast within the general mathematical framework. The paper also includes an evaluation of the FDD method in terms of both sensitivity and robustness.*

INTRODUCTION

Automated fault detection and diagnosis (FDD) has been successfully applied to critical systems, such as space exploration and nuclear power plants, in which early identification of small malfunctions would prevent loss of life and damage to equipment. HVAC systems often do not function as well as expected due to faults introduced during initial installation or developed during routine operation. In the late 1980s, some researchers investigated common faults and methods for FDD in simple vapor-compression cycles, such as household refrigerators (Stallard 1989). With the growing realization of the benefits brought by FDD, many publications related to HVAC FDD have appeared in the last decade (Comstock et al. 1999; Li 2004), and interest is increasing. According to the IEA ANNEX 34 final report (Dexter and Pakanen 2001), 23 prototype FDD performance monitoring tools and 3 validation tools have been developed, 30 demonstrations have taken place in 20 buildings, 26 FDD tools have been tested in real buildings, and 4 performance monitoring schemes have been jointly evaluated on 3 documented data sets from real buildings. Since 2001, 39 more papers have appeared (Li 2004). Overall, the literature can be summarized as follows.

- In terms of focus, the single largest focus of research has been on variable-air-volume (VAV) air-handling units (AHUs), accounting for 45% of the publications. Packaged air-conditioning systems come a distant second with 20% of the publications, and chiller systems have been the third focus at 18%. Rooftop and other packaged air conditioners are used extensively

Haorong Li is an assistant professor of architectural engineering at the University of Nebraska–Lincoln, Omaha, NE. **James E. Braun** is a professor of mechanical engineering at Purdue University, West Lafayette, IN.

throughout small commercial and institutional buildings, but compared to larger systems, they tend not to be well maintained. In addition, for both packaged and chiller systems, faults occur frequently in vapor-compression cycle equipment. Widespread application of automated FDD for vapor-compression cycle equipment will significantly reduce energy use and peak electrical demand, downtime, and maintenance costs.

- From the methodology point of view, there are three general approaches for FDD, namely, model-based, data-driven, and knowledge-based. Model-based methods use mathematical models often constructed from first principles. They are applicable to information-rich and modeling-manageable systems, where satisfactory models can be built in an affordable way to satisfy FDD application and enough sensors are available. Methods described by Rossi and Braun (1997), Siegel and Wray (2002), Shaw et al. (2002), Yoshida and Kumar (2001a, 2001b), and Dexter and Ngo (2001) fall into this category. The data-driven approach addresses FDD by means of directly processing a large amount of data to capture some meaningful statistics. It mainly applies to large-scale systems, such as the whole-building system, where it is difficult to construct an analytical model but heavy instrumentation is used and an exceptionally large amount of data is produced. Methods used by Riemer et al. (2002) and Reddy et al. (2003) can be classified in this category. The knowledge-based approach uses qualitative models that are based on causal analysis, expert systems, and/or pattern recognition. It is well suited for systems where, like the data-driven approach, detailed mathematical models are not available but, unlike the data-driven approach, a large amount of data is not available. The technique presented by Gerasenko (2002) is an example. Although all three FDD approaches have found their applications in HVAC systems, the model-based approach has been most used (Li 2004). This is because most HVAC systems are relatively small-scale, not heavily instrumented, and modeling-manageable.
- Most of the proposed techniques require either expensive system models or expensive measurements or both. For example, Rossi and Braun (1997) originally proposed the statistical rule-based (SRB) FDD technique and applied it to vapor-compression systems. This technique uses relatively low-cost sensors (nine temperature and one relative humidity) but requires an expensive system model, which entails a wide range of training data. Further reducing the implementation cost is vital for a practical FDD technique.
- Multiple simultaneous faults have barely been addressed in the literature. Most of the publications have only dealt with the presence of single faults. Breuker (1997) investigated the effect of two simultaneous faults on the performance of the SRB technique, which was developed for single faults. He used a simulation model and found that the presence of two simultaneous faults in a rooftop air conditioner did not result in the diagnosis of a third fault that was not present in the system. However, the diagnostic classifier was not capable of making multiple diagnoses, and some combinations of faults increased FDD sensitivity whereas others decreased sensitivity. Further investigations are warranted for testing more simultaneous faults under real operating conditions and for developing a methodology that can diagnose multiple faults.

The goal of the research described in this paper was to develop a low-cost diagnostic methodology for handling multiple simultaneous faults in vapor-compression cycle systems with emphasis on packaged air conditioners. This paper first formulates model-based FDD techniques in a general mathematical way and finds that the methodology of decoupling is the key to handling general multiple-input and multiple-output issues. In order to apply the decoupling methodology to noncritical HVAC&R systems, a physical decoupling methodology is developed that eliminates a cost-prohibitive overall system model. Finally, the method is implemented and evaluated in terms of both sensitivity and robustness.

MATHEMATICAL FORMULATION OF MODEL-BASED FDD

In a broad sense, all FDD approaches involve the use of quantitative or qualitative models. They can be either dynamic or steady-state, either physical or black-box or gray-box, either mathematical or linguistic. Mathematical models relate measured or derived states of the system to external inputs through the use of mathematical equations, while linguistic models, also known as *syntactic models*, describe the behavior of a system through the use of linguistic expressions such as logic sequences (e.g., fuzzy linguistic models). Since the majority of FDD approaches, especially for HVAC&R applications, are based on mathematical models, the following development is based on mathematical models. However, the development could be extended to linguistic models as well.

The thermodynamic states of a vapor-compression cycle are functions of external driving conditions and various faults, as shown in Figure 1a. It is important for FDD not to misinterpret variations in thermodynamic state-variables caused by changes in the driving conditions for faults. If measurements are classified directly, the classification can be complicated to consider the effect of external driving conditions. In order to simplify classification and improve overall FDD performance, normal operation models are typically used to predict expected values for these measurements under normal operation in terms of measured external driving conditions. For any steady-state measurement, the difference between expected and actual measurement values (residuals) should have a zero mean when there are no faults (see Figure 1b) and a probability distribution that is a weak function of driving conditions but dominantly dependent on faults.

The input-output relationship of the system after being incorporated with a normal operation model (fault-free model) can be described approximately as follows:

$$Y = F(X) \tag{1}$$

where $X = [x_1, x_2, ..., x_n]^T$, $Y = y_1, y_2, ..., y_m]^T$, and $F(X) = [f_1(X), f_2(X), ..., f_m(X)]^T$. X is the fault vector, with each entry x_i representing a measure of the level for each fault. Y is the state variable residual vector, with each entry y_i representing a particular state-variable residual. $F(X)$ is a nonlinear function vector with each individual nonlinear function $f_i(x_1, x_2, ..., x_n)$ defining the relationship between different faults at different levels, the state-variable residual Y; n is the number of fault types considered; and m is the number of chosen state variables.

After a normal model is incorporated, FDD is simplified to deal with only faults and normal variations in residuals independently. In a broad sense, this is the first occurrence of decoupling,

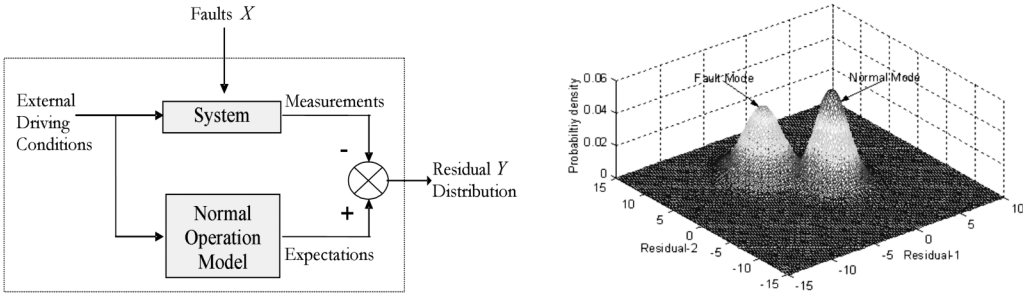

(a) System incorporated with a normal operation model (b) 2-dimensional residual distribution

Figure 1. Role of models in FDD: (a) system incorporated with a normal operation model and (b) two-dimensional residual distribution.

which is between faults and driving conditions. Typically, FDD is achieved by two separate steps—fault detection and fault diagnosis.

Fault Detection

Fault detection, which is to indicate whether the system is normal or not, can be done essentially by determining whether the resulting Y in Equation 1 is zero or not in a statistical sense. The tool used to achieve fault detection is termed the *fault detection classifier*. Although some quantitative fault diagnosis techniques can also do fault detection at the same time, implementing fault detection prior to attempting any diagnosis is recommended for the following reasons:

- Fault detection is much easier than fault diagnosis, and the probability for abnormal operation is lower than for normal operation. Therefore, the use of separate FDD steps can reduce computational requirement costs because the diagnosis step can be skipped when there are no faults.
- Fault detection can take statistical analysis into account easily, which makes the fault diagnosis method more flexible.

Original SRB Fault Detection Classifier. Rossi and Braun (1997) proposed a way to evaluate whether Y is zero indirectly by looking into the overlap (see Figure 1b) of the actual distribution and the expected distribution of the residual(s). When the overlap of the actual distribution and the expected distribution of the residual(s) decreases to a preset value (the classification error threshold), a fault is considered to be present.

The direct numerical integration of this overlap for high-dimensional (e.g., seven-dimensional for our case) probability distributions cannot be performed in real time on a microprocessor. Therefore, to obtain the analytical solution of overlap, Rossi and Braun (1997) employed the concept of a Bayes classifier, also known as the *Bayes error* (Fukunaga 1990).

The other merit of this classifier is that it converted the classification of an individual observation Y among infinite predefined classes ω_1, ω_2, ..., ω_n, ... inversely into identification of whether any class ω_i deviating from the normal operation appears using a series of observations Y_1, Y_2, ..., Y_n with certain overlap and let the fault diagnosis classifier separate different faults.

Since it is impracticable, if not impossible, to estimate the high-dimensional covariance matrix of the current operation online, an identical covariance matrix with that of normal operation is assumed. However, if this assumption is not well grounded, it may undermine the fault detection performance because the overlap is highly dependent on the covariance matrix. It is really difficult to evaluate the identical covariance matrix assumption because a large data set is necessary to estimate a high-dimensional covariance matrix with reasonable accuracy. However, it can be evaluated indirectly by checking the variance of individual variables. According to the experimental data collected by Breuker and Braun (1998):

- Faults have significant impact on the variance of state variables. For example, variances of subcooling, superheating, and evaporating temperature increase when the system has a refrigerant leakage fault (Li and Braun 2003).
- Different faults have different impacts. For example, refrigerant leakage has a larger impact on the variance of subcooling than evaporator fouling (Li and Braun 2003).

As a result of these considerations, a new fault detection classifier—one that does not require a faulty operation covariance matrix—was developed; it is described in the next section.

Normalized Distance Fault Detection Classifier. Li and Braun (2003) presented the development of a simple fault detection classifier that can be used for both individual and multiple simultaneous faults. The classifier evaluates the following inequality:

$$(Y - M_{normal})^T \Sigma_{normal}^{-1} (Y - M_{normal}) \underset{\omega_2:Faulty}{\overset{\omega_1:Normal}{\lessgtr}} (\chi^2)^{-1}\{(1-\alpha), m\} \quad (2)$$

where $(Y - M_{normal})^T \Sigma_{normal}^{-1} (Y - M_{normal})$ is the normalized distance, $(\chi^2)^{-1}\{(1 - \alpha),m\}$ is the threshold of normalized distance for normal operation, $(\chi^2)^{-1}\{,\}$is the inverse of the Chi-square cumulative distribution function, α is the false alarm rate, and m is the degree of freedom or dimension that is equal to the number of chosen state variables. Class ω_1, normal operation, is selected if the left-hand side is less than the right-hand side, and class ω_2, faulty operation, is selected otherwise. Due to modeling error, M_{normal} is not exactly zero, so Equation 2 takes modeling error into account to statistically evaluate whether Y is zero or not.

The above fault detection scheme can be illustrated using Figure 2. The residual distribution of normal operation can be characterized in terms of the covariance matrix Σ_{normal} and mean vector M_{normal} and depicted in the residual space plane as in Figure 2. In the residual space plane, any operating states (points) outside the normal operating region are classified as faulty while those inside the normal operation region are classified as normal. The normal operating ellipse is the fault detection boundary, which is determined by M_{normal}, Σ_{normal}, m, and α.

By contrast with the original SRB fault detection classifier, this normalized distance fault detection classifier is more robust in that it eliminates faulty operation information and only uses normal operation information, such as the normal mean and normal covariance matrix. Practically, normal operation information is more accessible and more reliable compared to faulty operation data. In addition, this scheme is intuitive in that the opposite of normal operation is abnormal operation. If the current operation point is not inside the normal operation region at a certain confidence according to reliable prior information, it should be classified as a faulty operation. Another advantage is that the fault detection decision is based on individual points rather than on a distribution, so it is more computationally efficient for online application.

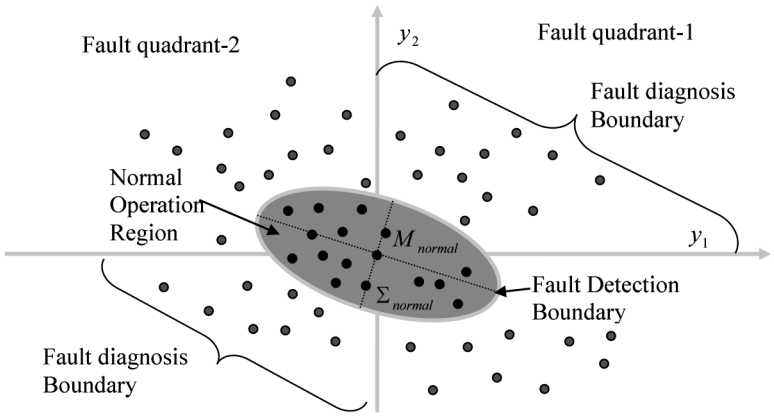

Figure 2. Illustration of FDD strategy.

Fault Diagnosis

Fault diagnosis, which entails the determination of the kind and location of the detected fault from a list of possibilities, needs to use the resulting Y (knowns) to find the causes X (unknowns) qualitatively or quantitatively. The nonlinear Equation 1 cannot get unique solutions for X for a given Y if $m < n$ and may result in inconsistencies if $m > n$, but it would not lose any generality to assume $m = n$. If $F(X)$ is known, multiple simultaneous fault diagnosis becomes easy. However, it is very difficult, if not impossible, to find $F(X)$. To simplify Equation 1, the first two items of Maclaurin's series can be used to linearize the nonlinear equation as follows:

$$Y = F(0) + \frac{\partial F}{\partial X}(0)(X - 0) = JX \tag{3}$$

where $F(0) = 0$ and

$$J = \frac{\partial F}{\partial X}(0) = \begin{bmatrix} \frac{\partial f_1}{\partial x_1} & \frac{\partial f_1}{\partial x_2} & \cdots & \frac{\partial f_1}{\partial x_n} \\ \frac{\partial f_2}{\partial x_1} & \frac{\partial f_2}{\partial x_2} & \cdots & \frac{\partial f_2}{\partial x_n} \\ \vdots & \vdots & \ddots & \vdots \\ \frac{\partial f_n}{\partial x_1} & \frac{\partial f_n}{\partial x_2} & \cdots & \frac{\partial f_n}{\partial x_n} \end{bmatrix}$$

is the Jacobian matrix of $F(X)$ evaluated at 0. Compared to $F(X)$, J is much easier to estimate by experiment, which requires n^2 tests. After J is estimated, diagnosis can be done more easily by

$$X = J^{-1}Y. \tag{4}$$

It should be pointed out that a nonsingular matrix J is a necessary and sufficient condition for the above equation. For a practical engineering problem, this condition is readily guaranteed if the given set of state variables Y can be used to uniquely describe the system under the possible fault vector X. It is not difficult at all to find such a set of state variables Y with the help of physical knowledge.

Original SRB Fault Diagnosis Method. Although J can be estimated approximately by experiment, it is still not generic because different units of the same type may have different values of J. Estimation of J for individual systems is only practical for large or critical systems. Instead of estimating J, the rule-based FDD method proposed by Rossi and Braun (1997) is equivalent to using the sign of J to do fault diagnosis.

$$J_{sign} = sign(J)$$

where *sign*() is the signum function (also called *sign function*), which extracts the sign of a real number. If faults occur individually, for example, only individual fault i happens at some time.

$$X_{sign} = sign(X) = sign([0, \ldots, x_i, \ldots, 0]^T) = [0, \ldots, 1, \ldots, 0]^T$$

and then

$$Y_{sign} = J_{sign}X_{sign} = sign\left(\left[\frac{\partial f_1}{\partial x_i}, \frac{\partial f_2}{\partial x_i}, \ldots, \frac{\partial f_n}{\partial x_i}\right]^T\right)$$

So, if a fault happens individually, for a given matrix J_{sign}, Y_{sign} is determined uniquely by X_{sign} and vice versa. Inversely, this can be used to do fault diagnosis by comparing Y_{sign} with the column of J_{sign} in the statistical sense or mathematically by

$$X_{sign} = sign(J_{sign}^T Y_{sign} - [n, n, \ldots, n]^T) . \quad (5)$$

By determining which entry of vector X_{sign} is unity, the fault diagnosis classifier can make a decision. The advantages of this method are that (1) it is very easy to infer the J_{sign} accurately by n simple tests or from experience or qualitative knowledge, compared to n^2 well-designed tests to estimate J roughly; (2) J_{sign} is generic at least for the same type of system, compared to different Js for different systems because there is no linearization approximation for J_{sign}; (3) this method of diagnosis uses direction change pattern (sign) to convert an infinite classification problem (infinite number of fault levels for an individual type of fault) into a multiple classification one. The drawback is that it can only handle individual faults.

Corresponding to the SRB fault diagnosis terminology, J_{sign} is equivalent to the fault diagnosis rules (see Table 1), which are expressed as positive and negative changes in residuals so that each fault type corresponds to a unique quadrant of a multi-dimensional residual space. To decide which fault is the most probable is equivalent to identifying which quadrant the current measurement belongs to. Combined with the normal operating ellipse, coordinate axes form the fault diagnosis boundary (see Figure 2).

Similar to the fault detection classifier, Rossi and Braun (1997) proposed a fault diagnosis classifier to implement the rule-based diagnostic method that involves evaluating the probability of the current distribution within each fault quadrant. When the probability of the most likely fault class exceeds that of the second most likely class by a preset threshold (fault probability ratio threshold), a diagnosis is made. The merit of this classifier is that it maintains the merit of the SRB fault diagnosis method, converting an infinite classification problem into a multi-classification one. However, similar to the fault detection classifier, direct numerical integration of the high-dimensional (e.g., seven-dimensional for this case) probability distributions cannot be performed in real time using a microprocessor. Yet, unlike the detection classifier, it is impossible to find an analytical solution. Therefore, Rossi and Braun (1997) made an assumption that each dimension of the seven-dimensional density function is independent. In other words, the cross-terms of the current operation covariance matrix are removed. This assumption simplified the seven-dimensional integration into a multiplication of seven one-dimensional integrations.

Table 1. Fault Diagnosis Rules

Fault Type	T_{evap}	T_{sh}	T_{cond}	T_{sc}	T_{dis}	ΔT_{ca}	ΔT_{ea}
Refrigerant leakage	–	+	–	–	+	–	–
Compressor valve leak	+	–	–	–	–	–	–
Liquid restriction	–	+	–	+	+	–	–
Condenser fouling	+	–	+	–	+	+	–
Evaporator fouling	–	–	–	–	–	–	+

However, the independence assumption can undermine the classifier performance when the covariance matrix is not diagonal (Li and Braun 2003). To eliminate the independence assumption and improve fault diagnosis performance, a simple distance fault diagnosis classifier, which does not require integration of the probability distributions, was developed and validated by Li and Braun (2003). This method has good sensitivity for diagnosing faults and is relatively insensitive to the choice of parameters and different operating conditions over a wide range.

Decoupling-Based Fault Diagnosis Method. With the new FDD classifiers, the merits of the SRB FDD method are maintained and the performance of the SRB FDD method has been improved significantly (Li and Braun 2003), but it is still unable to handle multiple simultaneous faults.

In order to extend the easily implemented SRB fault diagnosis idea to handle multiple simultaneous faults, Equation 3 can be further transformed as follows:

$$PY = PJX$$

$$Z = \Lambda X = [\lambda_1 x_1, \lambda_2 x_2, \ldots, \lambda_n x_n]^T$$

where $\Lambda = PJ = Diag([\lambda_1, \lambda_2, \ldots, \lambda_n])$, $Z = PY$ is the transformed feature vector, and $P = \Lambda J^{-1}$ is the transformation matrix to make Λ diagonal. There exists an infinite number of transformation combinations of Λ, P, and Z that can be obtained by arbitrarily choosing a diagonal Λ if matrix J is non-singular (this can be guaranteed by proper choice of Y physically). This transformation decouples interactions among the different faults and makes each entry of the feature vector Z only correspond to a unique fault entry of the fault vector X and vice versa.

$$X = \Lambda^{-1} Z = \left[\frac{z_1}{\lambda_1}, \frac{z_2}{\lambda_2}, \ldots, \frac{z_n}{\lambda_n}\right]^T \tag{6}$$

To eliminate impacts of the linearization operation and the driving-condition-independence assumption on diagnosis, the signum operation is applied to both sides of Equation 6. Since Z, based on actual measurements or virtual estimates, is corrupted by measurement noise, system disturbances, and modeling errors, it should be statistically evaluated by the signum operation. So, the n-dimensional FDD problem has been decoupled to be n one-dimensional SRB FDD problems.

$$sign(X) = sign(\Lambda^{-1}) sign\_stat(Z)$$

where $sign\_stat(Z)$ is a signum operation of each entry (z_i) of matrix Z in a statistical sense, such that

$$sign\_stat(z_i) = \begin{cases} -1, & \text{if } \dfrac{(z_i - \mu_{i,normal})}{\sigma_{i,normal}} < -\sqrt{(\chi^2)^{-1}\{(1-\alpha),1\}} \\ 0, & \text{if } \dfrac{|z_i - \mu_{i,normal}|}{\sigma_{i,normal}} \le \sqrt{(\chi^2)^{-1}\{(1-\alpha),1\}} \\ 1, & \text{if } \dfrac{(z_i - \mu_{i,normal})}{\sigma_{i,normal}} > \sqrt{(\chi^2)^{-1}\{(1-\alpha),1\}} \end{cases} . \tag{7}$$

It can be seen that the signum operation of each entry (z_i) of matrix Z is equivalent to evaluating the one-dimensional fault detection classifier of Equation 2. Then,

$$X_{sign} = \left[\frac{sign\_stat(z_1)}{sign(\lambda_1)}, \frac{sign\_stat(z_2)}{sign(\lambda_2)}, \ldots, \frac{sign\_stat(z_n)}{sign(\lambda_n)}\right]^T. \quad (8)$$

Equation 8 can be easily used to do multiple simultaneous fault diagnosis. Although the impacts of the linearization operation and driving-condition-independence assumption on diagnosis are eliminated and multiple simultaneous fault diagnosis can be handled, *P* and *Z* depend on *J*. If *J* is not known, *P* and *Z* cannot be determined mathematically. Since there exists an infinite number of transformation combinations of Λ, *P*, and *Z*, from the mathematical viewpoint it can be supposed without proof that there exists at least one *Z* that has physical meaning. So, if some *Z* can be found physically or empirically, the sign of Λ can also be decided empirically. Consequently, the methodology to physically construct the decoupled feature vector *Z* becomes the key point of this approach. In addition to the previous advantages listed for the SRB fault diagnosis method, the decoupling-based diagnosis method:

1. Simplifies fault detection from a high-dimensional problem to *n* one-dimensional problems. Equation 2 boils down to the following *n* one-dimensional equations:

$$\frac{(z_i - \mu_{i,normal})^2}{\sigma^2_{i,normal}} \begin{matrix} \omega_1: Normal \\ \leq \\ > \\ \omega_2: Faulty \end{matrix} (\chi^2)^{-1}\{(1-\alpha),1\}$$

The above one-dimensional fault detection classifier has been implemented into Equation 7.

2. Can achieve with one step by evaluating Equation 8. So the fault diagnosis classifier is not required.
3. Overcomes the drawback of the SRB diagnosis method and handles multiple simultaneous fault diagnosis.
4. Becomes more generic and system-independent and does not require complicated rules that depend on the system.

Unilateral Decoupling Case

The methodology based on full decoupling can handle multiple simultaneous faults easily, but the criterion of full decoupling is not a necessary condition and can be lowered. There are practical reasons for lowering the full decoupling criterion. Although a physically decoupled feature vector *Z* can be found for a fault vector *X*, some features may be too expensive to use for a noncritical FDD application. For example, condenser airflow rate could be a unique decoupling feature for condenser fouling, but its measurement is too expensive. An alternative way to obtain this kind of feature is to estimate it using a virtual sensor, which may be corrupted by other faults. In other words, although fault *i* may not impact other faults' features z_j's ($j \neq i$), its feature z_i would be contaminated by another fault *j*'s ($j \neq i$). Therefore, only the coupling from *i* to *j* is broken while the one from *j* to *i* is not. The worse case that can be handled is described as

$$Z = LX = \begin{bmatrix} l_{11} & & & \\ l_{21} & l_{22} & & \\ \vdots & \vdots & \ddots & \\ l_{n1} & l_{n2} & \cdots & l_{nn} \end{bmatrix} \begin{bmatrix} x_1 \\ x_2 \\ \vdots \\ x_n \end{bmatrix}, \quad (9)$$

where the feature z_i would be impacted by faults *j* (<*i*) but not by those (>*i*).

A sequential FDD method, which is contrasted with the above simultaneous FDD technique, can be used to solve this case:

- **Step 1:** Do FDD on fault 1. Because feature z_1 is independent of any other faults, fault 1 can be detected and diagnosed independently. If fault 1 does not exist, go to the next step. Otherwise, don't go to the next step until either fault 1 is fixed if it is severe enough or the features that have been corrupted by this fault are modified according to this diagnosed fault in the virtual sensor. So,

$$z_1 = l_{11}x_1 \Rightarrow x_1 = \frac{z_1}{l_{11}} \Rightarrow x_{1,sign} = \frac{sign\_stat(z_1)}{sign(l_{11})} .$$

- **Step 2:** Do FDD on fault 2. After step 1 has been done, either $x_1 = 0$ (if fault 1 does not exist or is fixed) or $l_{21} = 0$ (after modification according to fault 1) can be guaranteed. So,

$$z_2 = l_{21}x_1 + l_{22}x_2 = l_{22}x_2 \Rightarrow x_2 = \frac{z_2}{l_{22}} \Rightarrow x_{2,sign} = \frac{sign\_stat(z_2)}{sign(l_{22})} .$$

If it exists, fix fault 2 if it is severe enough or otherwise modify the infected features.

⋮ ⋮

- **Step *i*:** Do FDD on fault *i*. After steps 1, 2, ..., $i - 1$ have been done, either $x_k = 0$ or $l_{ik} = 0$ (for $k < i$) is guaranteed. So,

$$z_i = l_{i1}x_1 + l_{i2}x_2 + ,\ldots, + l_{ii}x_i = l_{ii}x_i \Rightarrow x_{i,sign} = \frac{sign\_stat(z_i)}{sign(l_{ii})} .$$

If it exists, fix fault *i* if it is severe enough or otherwise modify the infected features.

⋮ ⋮

- **Step *n*:** Do FDD on fault *n*. After steps 1, 2, ..., $n - 1$ have been done, either $x_k = 0$ or $l_{nk} = 0$ ($k < n$) is guaranteed. If fault *n* exists and is severe enough, then fix it:

$$z_n = l_{n1}x_1 + l_{i2}x_2 + ,\ldots, + l_{nn}x_n = l_{nn}x_n \Rightarrow x_{n,sign} = \frac{sign\_stat(z_n)}{sign(l_{nn})}$$

DECOUPLING STRATEGY FOR FAULTS IN VAPOR-COMPRESSION AIR CONDITIONERS

Interactions

As depicted in Figure 3, an air conditioner can be represented as a black box that is driven by faults, disturbances, and overall system driving conditions, including T_{aoc}, T_{aie}, and ϕ_{aie}, and

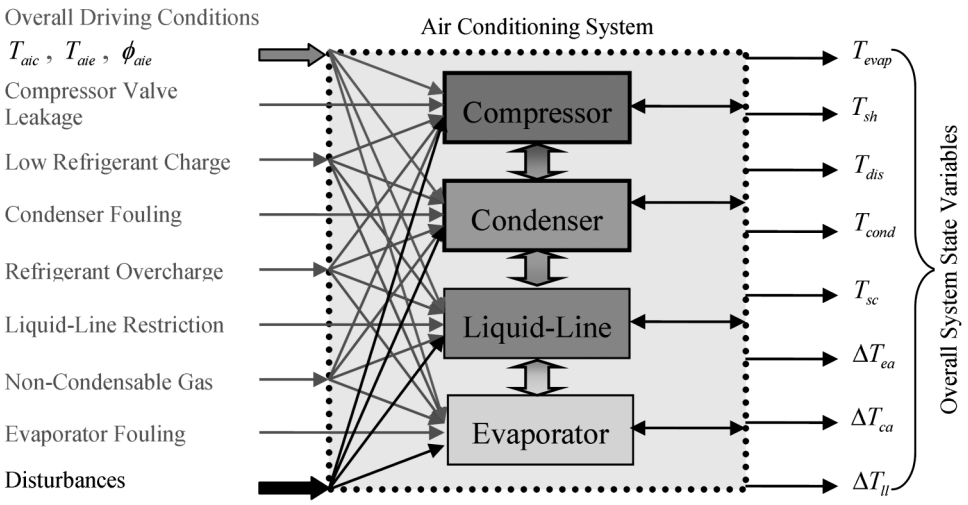

Figure 3. Fault interactions for air-conditioning systems.

outputs overall system state variables. It is difficult to tell which factors contribute to the current operation state directly from overall state variables. The SRB method uses normal state models to predict the normal operation states according to the overall driving conditions, generates residuals to decouple the interactions between driving conditions and faults, and also uses statistical analysis to further decouple the actions from disturbances but leaves the couplings among the different faults untouched. This is the reason SRB FDD methods cannot handle multiple simultaneous faults.

To handle multiple simultaneous faults, the interactions among different faults should be decoupled. That is, if one independent feature that is impacted by only one fault can be found for each individual fault, then multiple simultaneous faults are decoupled. It has been demonstrated that an infinite number of decoupled-feature sets can be constructed mathematically if detailed system models are available. Among the infinite number of decoupled-feature sets, some of them may have no physical meaning while the others may be physically intuitive, and some of them involve expensive measurements while the others are cost-effectively. However, detailed system models are expensive, sometimes cost-prohibitive, to develop, so an infinite number of decoupled-feature sets are difficult to achieve. The contribution of this mathematical derivation is that it provides a sure guide that decoupling is the key to handle multiple simultaneous faults. Those with intuitive physical meaning can be identified using an alternative way to a mathematical transformation, and, therefore, detailed system models are not necessarily entailed. For HVAC systems, detailed system models are cost-prohibitive, so only those with intuitive physical meaning and those that are readily available (low-cost) are practical. That is, there is an important and practical restriction for the independence features. They should be able to be expressed as functions of low-cost measurements such as temperature and pressure. This section develops a methodology or guidelines to find these kinds of features.

Generally speaking, a problem could be approached microscopically or macroscopically or both to obtain required results with different details. A macroscopic approach uses external and overall information to interpret the observed phenomenon or predict a coming phenomenon, while a microscopic approach uses internal and component information to interpret or predict a phenomenon. In some situations, a macroscopic approach is preferred and unnecessary details

are often ignored to simplify a complicated problem into a manageable one at the cost of losing some information. For example, statistical thermodynamics considers physical models at the level of particles while classical thermodynamics focuses on macroscopic and overall behavior of the particle system. FDD is not an exception: it can be approached either microscopically or macroscopically. The original SRB method approaches the FDD problem from the overall system perspective. It considers the thermodynamic impact of different faults on overall system state variables and uses overall system models to predict normal operation state variables according to the overall system driving conditions and then statistically evaluates the overall system state residuals to do FDD. The merit of this method is that it is simple and systematic, while the drawback is that it has difficulty handling multiple simultaneous faults and also depends on components that constitute the system. Multiple simultaneous faults have almost infinite combinations with different fault types and levels, and each combination has an overall impact on the overall system behavior. So it is almost impossible to extract so many system-level rules to do FDD with multiple simultaneous faults. In addition, system-level rules depend on the composition or structure of the system. So these two drawbacks are inherent to the SRB FDD method. Similar to the SRB FDD method, the derivation of the mathematical decoupling approach is also based on overall system models so, although it leads to an infinite number of decoupling cases through transformation to handle multiple simultaneous faults, it is not practical to implement. To overcome these drawbacks, an approach is developed that is based on individual component modeling and various conceptual or physical decoupling, which leads to the identification of decoupled features.

Taxonomy of Faults

Taxonomy always is based on and also conversely contributes to the understanding of a subject. By definition, taxonomy is "the study of the general principles of scientific classification" according to *Merriam-Webster Online* (Merriam-Webster 2006). Essentially FDD is a scientific branch of pattern recognition or classification, so taxonomy is the fundamental of FDD. For the SRB FDD method, all the faults are treated equally and only the overall impacts of them on the overall system state variables are discriminated.

From the macroscopic and overall system point of view, the only discrimination among the seven faults of refrigerant leakage, compressor valve leakage, condenser fouling, evaporator fouling, liquid-line restriction, refrigerant overcharge, and noncondensable gas is the directional change of the overall system state variables' residuals. However, from microscopic and macroscopic points of view, the seven faults considered by the FDD method can be divided into two classes, component-level and system-level faults, which are shown in Figure 4. The characteristic of component-level faults is that their source impact can be confined to a component, and this source impact is independent of other faults locally. So, decoupling of component-level faults can be achieved by investigating their source impacts.

Some faults are introduced during initial installation or service, while some faults develop during operation. If classified from the view of fault cause, they can be divided into operational and service faults. If service faults can be detected, diagnosed, and repaired immediately after installation or service, they will not occur simultaneously with operational faults. Therefore, coupling between service faults and operational faults can be removed.

In addition, some faults express themselves differently under different operation modes (transient and steady-state modes), while others are insensitive to operation modes. So, in terms of fault pattern expression, faults can be divided into mode-sensitive and mode-insensitive faults. This classification method contributes to FDD development in that some faults can only be detected and diagnosed in a certain operation mode and some can be detected and diagnosed in any operation mode but at different costs.

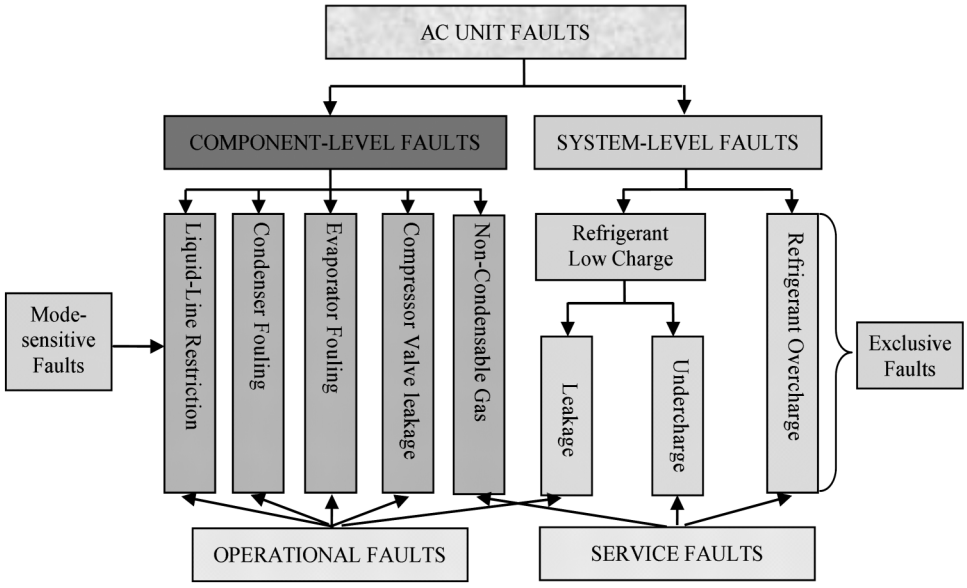

Figure 4. Taxonomy of air-conditioner faults.

Some faults can occur simultaneously, while some faults are mutually exclusive. For those mutually exclusive faults, there is no interaction or coupling among them so they are mutually decoupled in nature. In terms of fault relationship, faults can be divided into mutually exclusive and non-exclusive faults.

Compressor valve (or other internal) leakage is a component-level and operational fault. Although it impacts overall system state variables, such as discharge temperature and condensing temperature, these impacts are indirectly related to a compressor volumetric efficiency reduction, which is directly impacted by valve leakage. A loss of compressor volumetric efficiency results in a reduction of refrigerant flow rate and increasing specific compressor work, discharge pressure and temperature, and other changes of system variables, whose direction and intensity depend on the expansion device used. Physically, this source impact can be confined to the compressor component. Since a compressor valve is normally damaged when the system is running, it is classified to be an operational fault.

Condenser fouling (or fan degradation) is also a component-level fault. For an air conditioner, a direct impact of condenser fouling is the reduction of condenser airflow rate. A reduction of condenser airflow rate results in a heat transfer penalty that causes changes in state variables, whose direction and intensity depend on the expansion device used. For example, evaporator temperature would increase significantly for fixed orifice systems, but it would be almost unchanged for a thermostatic expansion valve (TXV) system until the fouling became very severe. A condenser fouling fault develops slowly when the system is running, so it is classified as an operational fault.

Similar to condenser fouling, evaporator filter and/or coil fouling (or fan degradation) is a component-level fault. For an air conditioner, a direct impact of evaporator fouling is the reduction of evaporator airflow rate. The reduction of evaporator airflow rate results in poorer heat transfer performance and causes changes in state variables, whose direction and intensity also depend on the expansion device used. For example, condenser temperature would decrease sig-

nificantly for fixed orifice systems, but it would be unchanged for a TXV system until the fouling became severe. Evaporator fouling is classified as an operational fault.

A liquid-line restriction fault often occurs in a dryer or a filter and can be classified as a component-level fault. This fault has the direct impact of increasing the pressure and possibly temperature difference between the inlet and outlet of the dryer or filter. The increased pressure drop also results in a series of changes in state variables, whose direction and intensity are highly dependent on the expansion device used. For example, for a system with a fixed orifice as the expansion device, a liquid-line restriction will result in a significant reduction of refrigerant flow rate, while a moderate liquid-line restriction will not result in a noticeable reduction of refrigerant flow rate when a TXV is used as the expansion device. This is because a TXV, an automatic control device, can compensate for an increased pressure drop resulting from a liquid-line restriction by increasing the opening of the TXV. Filter-driers continuously absorb water and dirt and become restricted over time, so a liquid-line restriction fault is classified as an operational fault. It has been found that a liquid-line restriction fault demonstrates a different pattern when the system is operating in transient mode than when operating in steady-state mode, so it is classified as a mode-sensitive fault.

Low or high refrigerant charge is a system-level fault because it can occur anywhere and its direct impact cannot be confined to a particular location. Refrigerant overcharge only happens during service, so it is a service fault. Low refrigerant charge has two possible causes: refrigerant is undercharged when service is done or there is a refrigerant leakage. Therefore, low charge can be a system-level operational or service fault. Low charge and high charge faults cannot occur simultaneously, so they are mutually exclusive faults.

Since air conditioners are under a positive gauge pressure system when charged, noncondensable gases can only be introduced during service. Noncondensable gases tend to accumulate in the condenser. The primary impact is to increase heat transfer resistance and results in high condensing pressures and temperatures. So, noncondensable gas is considered to be a component-level service fault.

In summary, the characteristic of a component-level fault is that its source impact is confined to a specific location or component and all the other impacts on the system originate from this source impact. On the contrary, the source impact of a system-level fault cannot be confined to a specific location or component. Operational faults usually develop during normal running and occur randomly or gradually, while service faults are introduced with service.

Summary of Decoupling Features for Rooftop Unit System Faults

Based on the above guidelines, Li and Braun (2006) developed decoupling features and virtual sensors for vapor-compression air conditioners. Figure 5 depicts the overall scheme that provides decoupling among component-level faults, among system-level faults, and between system-level and component-level faults. The decoupling can be summarized as follows:

- ΔT_{cond}, the condenser temperature residual, is used as a pseudo-decoupling feature for noncondensable gas; it is the difference between condenser temperature and saturation temperature corresponding to the condenser pressure when the system is off.
- $\Delta \dot{V}_{ca}$, the condenser volumetric airflow rate residual, is independent of any faults except for condenser fouling, so it serves as a decoupling feature for condenser fouling; it is the difference between the normal value and the estimated value of the condenser volumetric airflow rate.
- Similar to $\Delta \dot{V}_{ca}$, $\Delta \dot{V}_{ea}$, the evaporator volumetric airflow rate residual, is the decoupling feature for evaporator fouling; it is the difference between the normal value and the estimated value of the evaporator volumetric airflow rate.

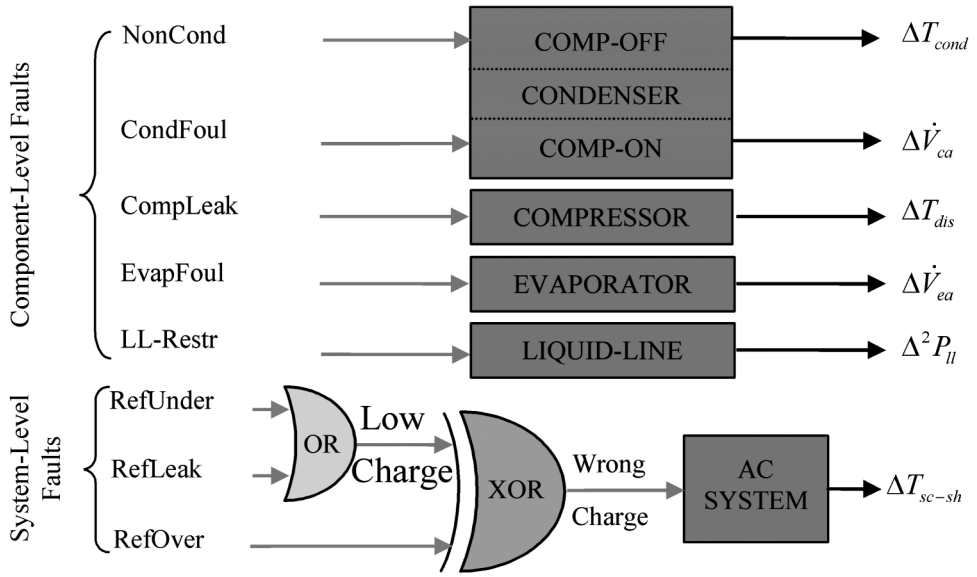

Figure 5. Decoupling scheme for air-conditioner faults.

- ΔT_{dis}, the discharge line temperature residual, is only dependent on compressor valve leakage fault, so it is used to break the coupling between compressor valve leakage and any other faults; it is the difference between the measured value and the estimated value from the compressor component model of the discharge line temperature.
- $\Delta^2 P_{ll}$, the liquid-line pressure drop residual, should be close to zero in a statistical sense except when there is a restriction in the liquid line and it is a decoupling feature for a liquid-line restriction.
- Low and high refrigerant charge faults are naturally decoupled because they cannot both exist at the same time; $\Delta T_{sc\text{-}sh}$, the weighed residuals of suction superheat and liquid-line subcooling, is a decoupling feature that depends uniquely on refrigerant charge and is independent of operating conditions and other faults.

A mathematical description of the decoupling scheme is presented in Equations 10 and 11. In Equation 10, each element of vector Z is a unique function of a unique fault. Through decoupling, the FDD problem has been converted to a series of one-dimensional fault detection problems. Although the fault diagnosis rules for each fault are straightforward, Equation 10 can be presented in a linearized form as shown in Equation 11 and the result used in combination with Equations 7 and 8 to perform FDD according to prescribed statistical thresholds. It is not actually necessary to perform a linearization. It is only necessary to know the sign of the constants within Z to perform diagnosis using the decoupling features and Equations 7 and 8. This method has the advantages of not requiring overall system models and utilizing features that are generic and system-independent.

$$Z = \begin{bmatrix} \Delta T_{sat} \\ \Delta T_{dis} \\ \Delta^2 P_{ll} \\ \Delta \dot{V}_{ca} \\ \Delta \dot{V}_{ea} \\ \Delta T_{sc-sh} \end{bmatrix} = F(X) = \begin{bmatrix} f_1(NonCond) \\ f_2(CompLeak) \\ f_3(LLRestr) \\ f_4(CondFoul) \\ f_5(EvapFoul) \\ f_6(RefCharge) \end{bmatrix} \tag{10}$$

$$Z = \begin{bmatrix} \Delta T_{sat} \\ \Delta T_{dis} \\ \Delta^2 P_{ll} \\ \Delta \dot{V}_{ca} \\ \Delta \dot{V}_{ea} \\ \Delta T_{sc-sh} \end{bmatrix} \approx \Lambda X = \begin{bmatrix} \lambda_1 & & & & & \\ & \lambda_2 & & & & \\ & & \lambda_3 & & & \\ & & & \lambda_4 & & \\ & & & & \lambda_5 & \\ & & & & & \lambda_6 \end{bmatrix} \begin{bmatrix} NonCond \\ CompLeak \\ LLRestr \\ CondFoul \\ EvapFoul \\ RefCharge \end{bmatrix} \tag{11}$$

VALIDATION

Figure 6 depicts different models and their inputs and outputs for the FDD method. The inputs include both actual measurements (circled symbols) and variables determined from virtual sensors or simple combinations of actual measurements (bare symbols). The outputs are decoupled features (symbols within shaded ovals) and virtual sensor outputs needed by other modules. Many of the features and virtual sensors rely on quasi-steady performance. Quasi-steady state is a condition where the state variables are close to their equilibrium values for a given set of external driving conditions. A steady-state detector is required for implementation of this FDD method.

The FDD method considers important and difficult-to-diagnose faults that impact system cooling capacity, efficiency, and equipment life as documented by Breuker and Braun (1998), including faults that degrade compressor flow capacity (e.g., compressor valve leakage), low or high refrigerant charge (leakage or inadequate charging during service), air-side fouling or loss of flow for the condenser or evaporator, liquid-line restriction (e.g., filter/dryer clogging), and presence of a noncondensable gas.

For the evaluations in this paper, the FDD method was applied in a post-processing mode after data were collected. The combination of slope and variance methods (Li and Braun 2003) was used to determine quasi-steady conditions for the data sets that were obtained. In addition to the measurements shown in Figure 6 (circled symbols), compressor power was measured for the purpose of evaluating fault impact. Cooling capacity was calculated from measured states and a virtual sensor for refrigerant flow (see Li and Braun [2006]). Only the steady-state method for liquid-line restriction faults was employed as described by Li and Braun (2006). Improved FDD performance for this fault would undoubtedly be achieved using the transient method of Li and Braun (2006). However, this method was not available at the time testing was performed and therefore no transient data are available. In addition, noncondensable gas faults were not considered. A simple diagnostic classifier was employed with a normalized fault indicator defined as

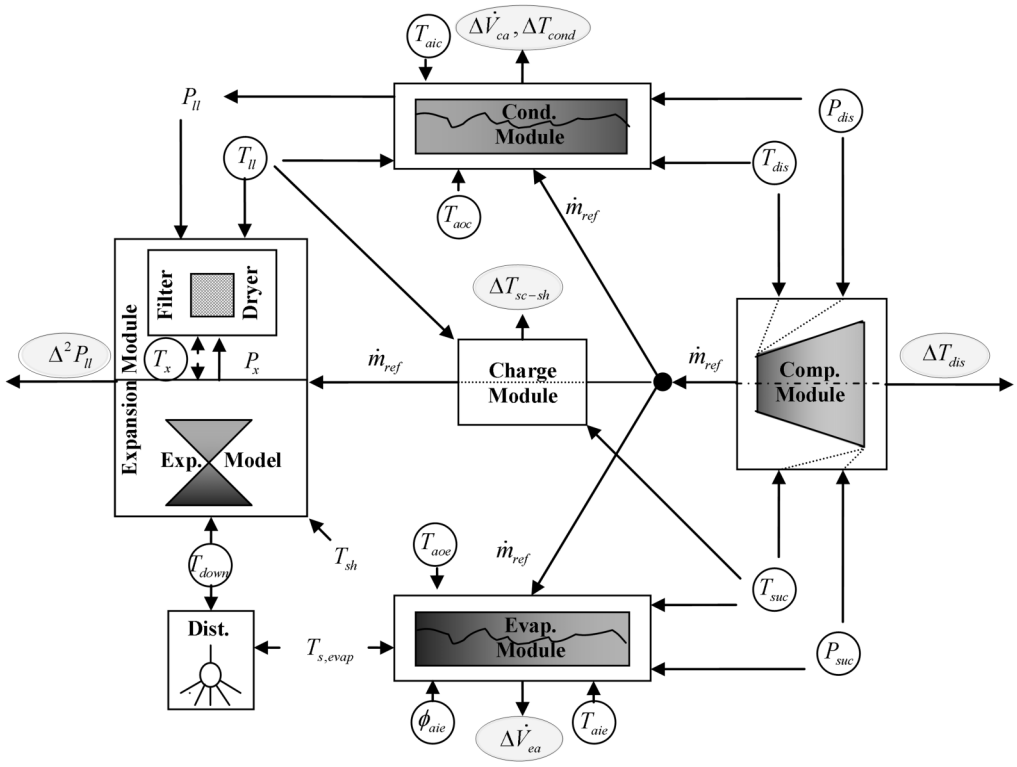

Figure 6. FDD modules and their inputs and outputs.

$$IND_{faultname} = \frac{fv_{current}}{fv_{range}},$$

where $IND_{faultname}$ denotes the decoupling fault feature for a given fault (*faultname*), $fv_{current}$ denotes the current feature value, and fv_{range} is a predefined range of interest for the feature value. For results presented in this paper, fv_{range} was chosen as the feature value at an individual fault level causing approximately a 20% cooling capacity degradation. FDD thresholds for the normalized indicators were at 0.2 (i.e., approximately 4% capacity degradation). The method can generally diagnose faults at lower levels, but at lower levels the fault impact is thought to be insignificant. Table 2 summarizes values for fv_{range} that were employed in this study.

FDD SENSITIVITY AND ROBUSTNESS

A 5-ton rooftop unit having a SEER of about 11 was installed at Purdue University to evaluate performance of the FDD method. This unit uses a TXV as the expansion device and has a fixed-speed, hermetically sealed scroll compressor. The evaporator blower uses a direct-drive motor with three speed options (nominal flow rate is 2000 cfm for the middle speed option), while the condenser fan is single-speed with a nominal flow rate of 4500 cfm. The condenser has five parallel condensing circuits and one subcooling circuit, while the evaporator is composed of seven parallel evaporating circuits. The standard system charge is 9 lb, 8 oz R-22. The measurements used for FDD tests are:

- Temperature measurements: evaporating temperature, suction line temperature, discharge line temperature, condensing temperature, liquid-line temperatures before and after filter/drier temperature, expansion device downstream temperature, air temperatures of the condenser inlet and outlet, and dry-bulb temperature and relative humidity of the mixed air.
- Refrigerant pressure measurements: suction line pressure and discharge line pressure for the compressor.
- Power transducer to measure power consumption of the compressor.

Table 3 tabulates the method of implementing faults and corresponding fault levels simulated. Six faults were implemented in the Purdue field site: compressor valve leakage (CompLeak), condenser fouling (CondFoul), evaporator fouling (EvapFoul), liquid-line restriction (LLRestr), refrigerant undercharge (RefLow), and refrigerant over charge (RefHigh). Five fault levels were introduced for refrigerant charge and compressor leakage faults, and four fault levels were introduced for the other three faults. Since tests were performed in a field setting, the driving conditions were uncontrollable. Typically, they were conducted in the afternoon (from around 1:30 p.m. to 8:00 p.m.) when there was no direct solar radiation striking the condenser or its air outlet sensors. Most of the tests were performed in the summer and fall of 2003, and some of them were conducted in the spring of 2004.

Sensitivity

The sensitivity of the FDD technique is defined as the lowest fault level introduced to the system that could be successfully detected and diagnosed (the diagnostic thresholds of Table 2 were not employed). Below these levels, the FDD method could not reliably diagnosis faults. Since there are infinite combinations of multiple faults with different fault levels, sensitivity was only

Table 2. Predefined Feature Values and FDD Thresholds

Fault Name	CompLeak	CondFoul	EvapFoul	LLRestr	RefLow	RefHigh
Feature	ΔT_{dis}	$\Delta \dot{V}_{ca}$	$\Delta \dot{V}_{ea}$	$\Delta^2 P_{ll}$	ΔT_{sc-sh}	ΔT_{sc-sh}
fv_{range}	8.3 (°C)	$0.25\dot{V}_{ca,setting}$	$0.25\dot{V}_{ea,setting}$	4.4 (bar)	5.6 (°C)	5.6 (°C)
Threshold	0.2	0.2	0.2	0.2	0.2	–0.2

Table 3. Method of Implementing Faults and Corresponding Fault Levels Simulated

Fault	**Fault Introduction Method**	**Fault Level Expression**	**Fault Level Simulated**					
			0	**1**	**2**	**3**	**4**	**5**
CompLeak	Partially open a bypass valve between discharge and suction lines	% refrigerant mass flow rate bypass	0%	8%	18%	33%	44%	56%
CondFoul	Partially block condenser airflow with paper	% reduction of air volume flow rate	0%	3%	10%	13%	16%	N/A
EvapFoul	Partially block evaporator airflow with paper	% reduction of air volume flow rate	0%	5%	9%	16%	31%	N/A
LLRestr	Partially close the needle valve on the liquid line	% of the pressure drop from high to low sides	0%	5%	10%	13%	19%	N/A
RefLow	Undercharge the system	% reduction of charge	0%	11%	16%	21%	26%	32%
RefHigh	Overcharge the system	% increase of charge	0%	11%	16%	21%	26%	32%

evaluated for individual faults. The implementation of each fault at different levels of Table 3 took from three to four hours in a single afternoon and driving conditions changed. However, there were no drastic changes in temperature and humidity. Therefore, although sensitivities in terms of physical level were stable, sensitivities in terms of performance degradation may have small variations due to the effects of driving conditions.

Table 4 summarizes the FDD sensitivity results. The levels at which faults could be diagnosed are expressed in several different ways: (1) fault level (from Table 3), (2) physical level (from Table 3 definitions), (3) percent degradation in unit cooling capacity, (4) percent degradation in unit EER, and (5) percent degradation in unit sensible heat ratio (SHR). Since the fault levels were introduced at discrete levels, the first level represents the best possible sensitivity for these tests. The method could detect low refrigerant charge and loss of compressor performance at the lowest levels introduced and all other faults at the second level. All of the faults could be reliably diagnosed before a 5% degradation in capacity, EER, or SHR.

False alarm is an indication of a fault when in actuality a fault has not occurred. For a given technique, there is an inherent trade-off between minimizing the false alarms and maximizing sensitivity. Table 5 lists the theoretical false alarm rates calculated from the fault indicator standard deviation at the FDD thresholds. Except for the liquid-line restriction, the faults had very small false alarm rates. Since the sensitivity of liquid-line restriction is high, it seems that there is some potential to reduce its false alarm rate by means of raising the FDD threshold. However, robustness tests show that it is impractical to raise the FDD threshold for the liquid-line restriciton.

Robustness

To verify robustness, multiple simultaneous fault combinations of six faults were considered. Only one fault level was implemented for each combination because there are infinite combinations if fault level is considered. Except for compressor leakage, the faults were implemented at the levels between the first diagnosed and next levels (see Table 6). Compressor leakage was implemented at different and relatively high fault levels because (1) a compressor leakage fault is completely decoupled from the other faults and has the highest robustness

Table 4. FDD Sensitivity for Individual Faults

Fault	Simulated Level	Physical Level	Capacity Degradation	EER Degradation	SHR Degradation
CompLeak	1st	8%	5%	3%	–3%
CondFoul	2nd	10%	3%	4%	0%
EvapFoul	2nd	9%	5%	4%	4%
LLRestr	2nd	10%	3%	1%	2%
RefLow	1st	11%	3%	1%	5%
RefHigh	2nd	16%	2%	2%	0%

Table 5. Fault Indicator Standard Deviations of Normal Operations and False Alarm Rates

Fault Name	CompLeak	CondFoul	EvapFoul	LLRestr	RefLow	RefHigh
FDD Threshold	0.2	0.2	0.2	0.2	0.2	–0.2
Standard Deviation	0.072	0.074	0.091	0.133	0.066	0.066
False Alarm Rate	0.003	0.004	0.014	0.067	0.005	0.005

Table 6. Individual Fault Levels Implemented for Multiple Simultaneous Fault Tests

Test No.	CompLeak	CondFoul	EvapFoul	LLRestr	RefLow	RefHigh	Capacity Degradation	EER Degradation	SHR Degradation
1	27%	0	0	0	14%	0	28%	19%	–6%
2	27%	11%	0	0	14%	0	31%	25%	–9%
3	25%	11%	12%	0	11%	0	25%	20%	–6%
4	25%	11%	12%	12%	11%	0	27%	22%	–4%
5	0	11%	12%	12%	11%	0	9%	12%	14%
6	0	0	12%	12%	11%	0	5%	4%	12%
7	0	0	0	12%	14%	0	5%	0%	10%
8	29%	0	0	12%	14%	0	30%	21%	–6%
9	25%	0	12%	12%	11%	0	26%	17%	–2%
10	25%	0	12%	0	11%	0	25%	17%	0%
11	0	0	12%	0	11%	0	4%	1%	10%
12	0	11%	12%	0	11%	0	5%	9%	8%
13	0	11%	0	0	14%	0	6%	7%	4%
14	0	11%	0	12%	14%	0	6%	6%	10%
15	29%	11%	0	12%	14%	0	29%	23%	–7%
16	32%	11%	0	0	0	0	34%	28%	–18%
17	21%	11%	12%	0	0	0	25%	21%	–2%
18	21%	11%	12%	12%	0	0	21%	17%	–3%
19	0	11%	12%	12%	0	0	6%	10%	9%
20	0	0	12%	12%	0	0	1%	0%	8%
21	19%	0	12%	12%	0	0	21%	14%	–2%
22	32%	0	0	12%	0	0	33%	24%	–15%
23	0	11%	0	12%	0	0	-3%	4%	2%
24	32%	11%	0	12%	0	0	28%	25%	–15%
25	0	11%	12%	0	0	0	6%	10%	6%
26	19%	0	12%	0	0	0	20%	13%	–5%
27	33%	0	0	0	0	21%	30%	23%	–16%
28	32%	11%	0	0	0	21%	28%	24%	–17%
29	35%	11%	16%	0	0	21%	39%	35%	–9%
30	35%	11%	16%	12%	0	21%	36%	33%	–9%
31	0	11%	16%	12%	0	21%	8%	15%	8%
32	0	0	16%	12%	0	21%	7%	8%	9%
33	0	0	0	12%	0	21%	–3%	–1%	0%
34	32%	0	0	12%	0	21%	32%	25%	–13%
35	35%	0	16%	12%	0	21%	38%	31%	–6%
36	35%	0	16%	0	0	21%	38%	31%	–7%
37	0	0	16%	0	0	21%	7%	8%	8%
38	0	11%	16%	0	0	21%	8%	15%	7%
39	0	11%	0	0	0	21%	3%	10%	–1%
40	0	11%	0	12%	0	21%	3%	11%	1%
41	32%	11%	0	12%	0	21%	34%	31%	–16%

Table 7. Fault Indicators for the Different Faults

Fault	CompLeak	CondFoul	EvapFoul	LLRestr	RefLow	RefHigh
Indicator Number	1	2	3	4	5	6

Table 8. Normalized Fault Indicator Error and Its Meaning

Case	$\lvert\rho_i\rvert < 1$	**When it is Normal**		**When it is Faulty**	
		$\rho_i \le -1$	$\rho_i \ge 1$	$\rho_i \le -1$	$\rho_i \ge 1$
RefHigh	OK	False alarm	False alarm	Sensitivity gain	Wrong Diagnosis
RefLow		False alarm	False alarm	Wrong Diagnosis	Sensitivity gain
Other Faults		OK	False alarm	Sensitivity loss	Sensitivity gain

while other faults are unilaterally decoupled from it, (2) various compressor leakage faults are required to test the fault evaluation algorithm, and (3) high levels of compressor leakage faults are better for robustness tests of other faults. Fault levels of condenser fouling, liquid-line restriction, and refrigerant overcharge were fixed, while two fault levels of low refrigerant charge and evaporator fouling were simulated and compressor leakage fault levels ranged from 20% to 35%. Since refrigerant charge faults are mutually exclusive, the total number of combinations is the sum of those at low charge,

$$C_4^2 + C_4^3 + C_4^4 = 11 ,$$

and high charge,

$$C_4^1 + C_4^2 + C_4^3 + C_4^4 = 15 .$$

All 41 combinations with individual fault levels implemented are listed in Table 6. All of the possible 41 combinations were considered. For reference, indicators for the different faults are given in Table 7. Figure 7 shows the different combinations of faults implemented for the 41 different cases and also shows differences between binary indicators (1 = fault, 0 = no fault) for individual diagnosed and implemented faults. A −1 denotes a missed diagnosis or sensitivity loss for one fault and a 1 denotes a false alarm. There were and two missed diagnoses (lost sensitivity) two false alarms for combinations with a liquid-line restriction. As previously noted, only the steady-state method presented by Li and Braun (2006) was employed for liquid-line restriction. It is expected that the and missed diagnoses false alarms would be eliminated using the transient method of Li and Braun (2006).

In order to quantify the robustness, a normalized indicator error, ρ_i, is defined as

$$\rho_i = \frac{IND_{i,MSF} - IND_{i,SF}}{\left| IND_{i,SF} - \left| IND_{i,threshold} \right| \right|} ,$$

where i is the individual fault name, $IND_{i,SF}$ is the fault indictor of fault i occurring individually, $IND_{i,MSF}$ is the fault indicator of fault i occurring simultaneously with other faults, and $IND_{i,threshold}$ is the FDD threshold of fault i. Table 8 summarizes meanings of ρ_i for different cases.

Figure 8 plots the normalized fault indicator error for compressor leakage. It can be seen that there were no false alarms or sensitivity losses or gains. The normalized fault indicator error is much smaller for faulty operation than for normal operation, meaning that the fault indicator has very good robustness against noise and uncertainties and high sensitivity to faults. For faulty operation, the noise and uncertainties are suppressed by high sensitivity, meaning that it is less likely to have sensitivity loss for faulty operation. This confirms the prior theoretical analysis: compressor valve leakage fault is completely decoupled from the other faults.

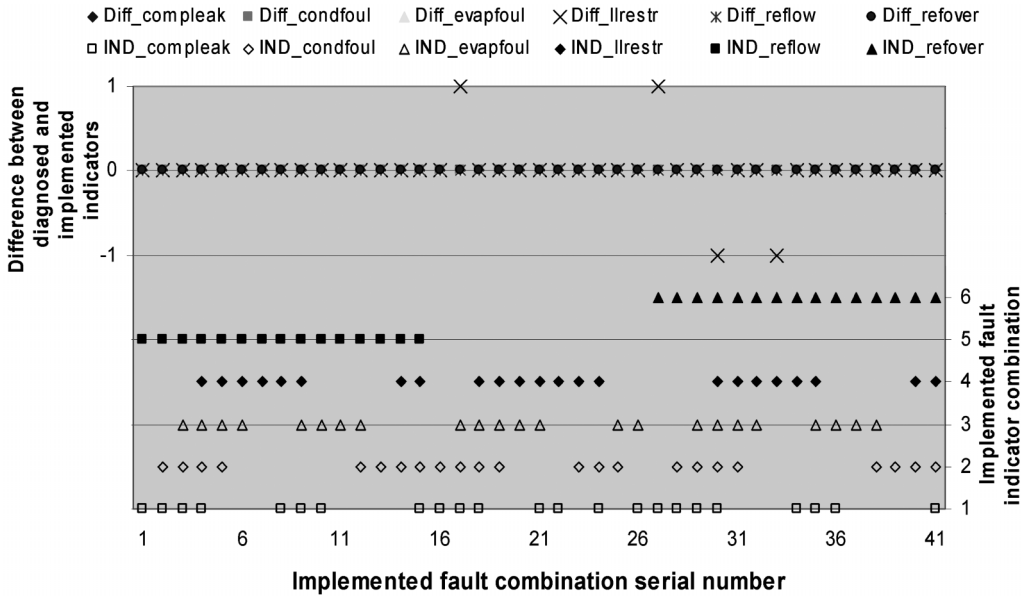

Figure 7. Robustness tests for multiple simultaneous FDD.

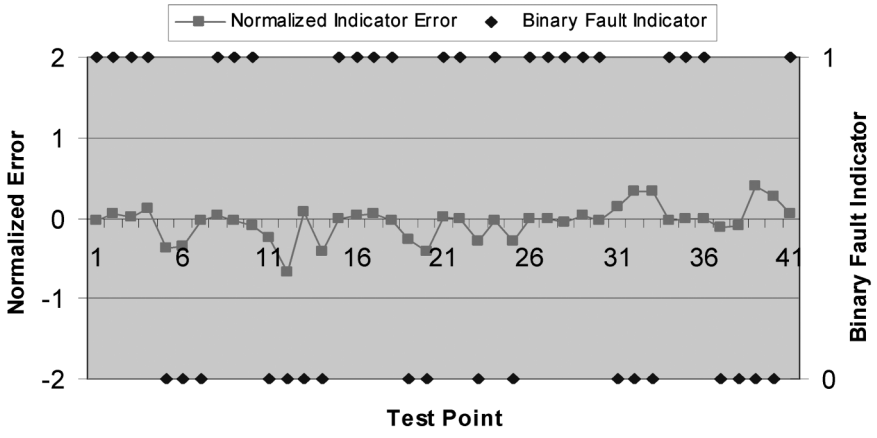

Figure 8. FDD robustness for compressor leakage.

The normalized fault indicator error for condenser fouling fault is given in Figure 9. It can be seen that all the points are within the robustness boundaries and there is no obvious difference in robustness between normal operation and faulty operation. Although there were no false alarms or sensitivity losses, robustness was not as good as for compressor valve leakage. There are two factors that affect condenser fouling robustness: refrigerant mass flow rate estimation and condenser outlet refrigerant enthalpy estimation. It seems that the compressor model and refrigerant mass flow rate correction algorithm have good performance. Theoretical analysis shows that if the condenser outlet refrigerant quality is larger than 0.1, the relative error in enthalpy estimation is less than 5%. If the refrigerant charge is more than 50% of the nominal value, the condenser outlet refrigerant quality will not be less than 0.1.

In Figure 10, the normalized fault indicator error for evaporator fouling is plotted. It can be seen that there is one point that is out of the range of the robustness boundaries and three points that are marginally within the boundaries. However, the point outside the lower boundary does

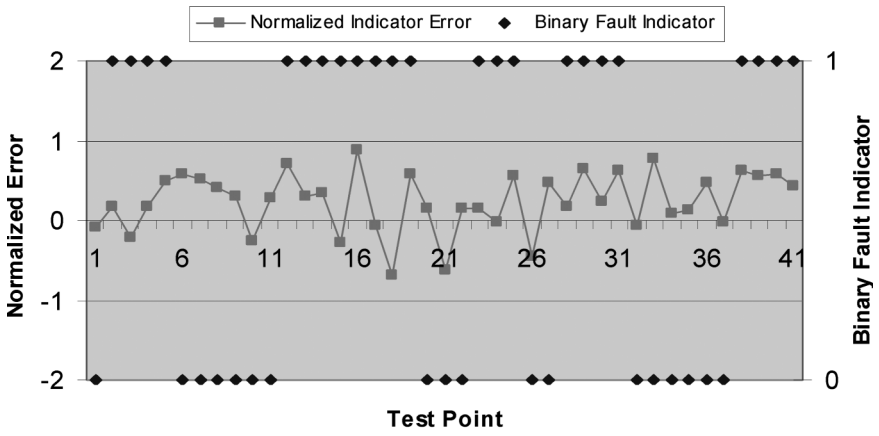

Figure 9. FDD robustness for condenser fouling.

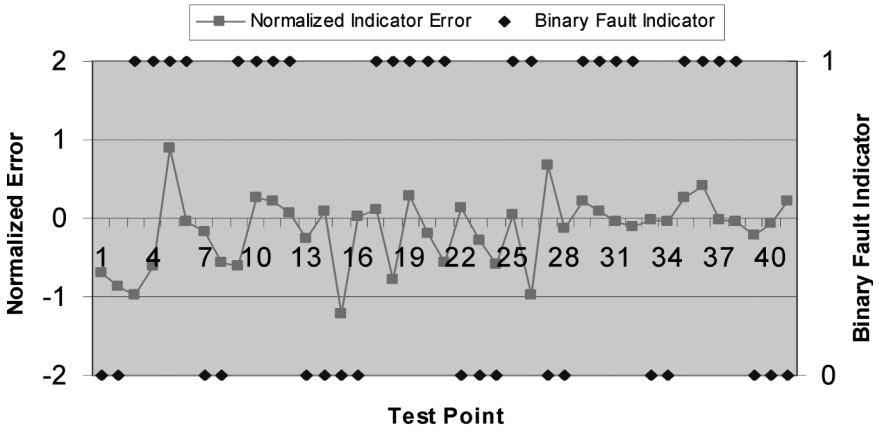

Figure 10. FDD robustness for evaporator fouling.

operate normally, so it will not cause any sensitivity loss. Overall, robustness for evaporator fouling was not as good as for compressor leakage and condenser fouling, but there were no false alarms or sensitivity losses. Three factors affect evaporator fouling robustness: refrigerant mass flow rate estimation, condenser outlet refrigerant enthalpy estimation, and evaporator outlet air enthalpy estimation. Since there is no humidity sensor for evaporator outlet air, its enthalpy is estimated using a virtual sensor, which adds some additional noise and uncertainty.

The normalized liquid-line restriction fault indicator error is shown in Figure 11. It can be seen that there are six points that are out of the robustness boundaries. Two of them operating normally are outside of the upper boundary and cause false alarms. Another two operating abnormally are outside of the lower boundary and cause sensitivity losses. The other two of them operating abnormally are outside the upper boundary and cause sensitivity gain. There are three points that are marginally within the boundary.

The reason for worse robustness is that more uncertainties are introduced: (1) refrigerant mass flow rate estimation, (2) condenser outlet refrigerant pressure estimation, and (3) estimation of pressure drop across the TXV. Pressure drop across the TXV is estimated using a TXV model that is sensitive to superheat measurement noise and refrigerant mass flow rate estimation. In addition, when the operation is out of the control range of the TXV, the TXV model will not have good performance. There are two situations where this will occur: (1) when the refrigerant charge is lower than a certain value, the TXV is saturated and will cause abnormally high superheat, and (2) when there is a compressor leakage fault, the evaporating pressure may be high enough to trigger the TXV maximum operation pressure. In addition to more uncertainties, the pressure drop across the clogged filter/drier itself varies according to refrigerant mass flow rate and refrigerant state even for the same physical fault level. As previously noted, it is expected that the false alarms and missed diagnoses would be eliminated if the transient method of Li and Braun (2006) were employed for liquid-line restriction faults.

The normalized fault indicator error for both refrigerant low and high charges is plotted in Figure 12. The binary fault indicator indicates undercharge by 1, nominal/normal charge by 0, and overcharge by –1. For the refrigerant low charge fault, there are three points that are outside the upper boundary, which indicates sensitivity gain, and there were no wrong diagnoses or sen-

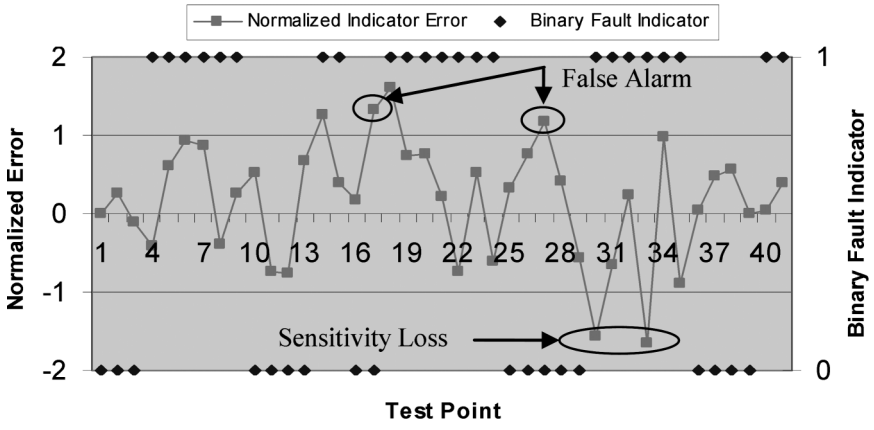

Figure 11. FDD robustness for liquid-line restriction.

sitivity losses. When the refrigerant is normally charged and overcharged, all the test points are within the robustness boundaries and there are no false alarms or sensitivity losses.

Table 6 tabulates all fault impacts for the different tests in terms of performance degradations in capacity, EER, and SHR. Some combinations of faults cause very significant performance impacts, therefore service would be justified. Generally, faults have a more significant effect on capacity than EER. The impact on SHR is even less than that on EER. However, in some cases faults increase latent removal (reduced SHR), which leads to increased cooling loads and greater operating costs. On the other hand, an increased SHR could lead to comfort problems.

CONCLUSIONS AND DISCUSSION

One of the unique and primary contributions of this paper is a mathematical framework for decoupling faults within the context of model-based diagnostic approaches. This framework provided a strong tool for development of a specific FDD approach for vapor-compression equipment that could handle multiple simultaneous faults. This problem had not been previously solved in a practical manner. However, the methodology is general and could be applied to a variety of different systems and FDD problems. The primary difficulty in attacking new problems is in identifying decoupling features that work well and are practical in terms of cost and implementation. The development for vapor-compression equipment relied heavily on the development of virtual sensors to reduce costs. In addition, the decoupling schemes included the use of simplified mathematical and non-mathematical decoupling approaches.

Decoupling based solely on mathematical transformation requires complicated and expensive system models and is not practical for noncritical applications. Casting the SRB FDD method within the context of the general mathematical framework led to an important incitement that significantly reduced the modeling requirements: it is only necessary to characterize the directional change in decoupling features in order to perform diagnostics. As a result, it is not necessary to have models that explicitly relate decoupled features to both operating conditions and faults—it is only necessary to have models that relate decoupled features for normal operating equipment to operating conditions and to have knowledge about the directional change in these features with faults. This requirement for mathematical decoupling is much less stringent and allows the use of much simpler models for decoupling features.

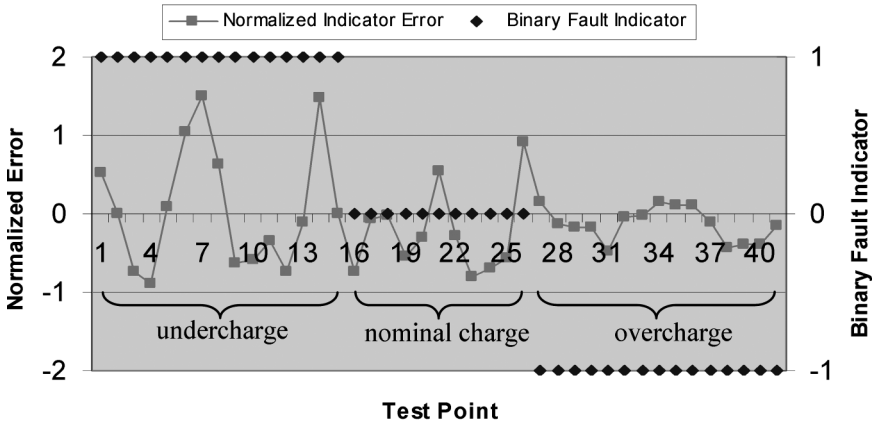

Figure 12. FDD robustness for refrigerant low and high charge faults.

Non-mathematical decoupling relies on an understanding of the physical system and service processes to decouple faults. For instance, some combinations of faults cannot possibly occur simultaneously (e.g., low and high refrigerant charges) and are naturally decoupled. Other faults can be decoupled based on how and/or when they occur. For example, introduction of a noncondensable gas or overcharging of refrigerant can only occur when the unit is serviced. As a result, additional measurements and techniques available to a service technician can be employed to diagnose these faults after initial service has been performed.

Based on the decoupling features and virtual sensors proposed by Li and Braun (2006), the proposed decoupling-based FDD method was implemented for vapor-compression systems. Faults were artificially introduced into a rooftop air conditioner at different levels in order to evaluate sensitivity and robustness of the method. Sensitivity tests showed that all of the individual faults can be identified before they cause 5% of degradation in cooling capacity, EER, and SHR. Robustness tests of 41 multiple simultaneous fault combinations showed that no wrong diagnosis occurred, with only two false alarms and sensitivity losses for a liquid-line restriction. The method presented in this paper was developed and validated for simple vapor-compression systems having fixed-speed fans and on/off compressor control. However, it can be readily extended to equipment having multiple stages of compression and fan speeds following the approach utilized in this work.

ACKNOWLEDGMENTS

This work was supported by the California Energy Commission (CEC) with additional cost-sharing provided by Honeywell, Inc., and Field Diagnostic Services, Inc.

NOMENCLATURE

α = false alarm threshold
CompLeak = compressor valve leakage
CondFoul = condenser fouling
$\Delta^2 P_{ll}$ = liquid-line filter/drier pressure difference residual
ΔT_{ca} = condenser air temperature difference
ΔT_{cond} = condensing temperature residual
ΔT_{dis} = discharge line temperature residual
ΔT_{ea} = evaporator air temperature difference
ΔT_{ll} = temperature difference across the liquid-line filter-drier
$\Delta T_{sc\text{-}sh}$ = refrigerant charge diagnosis feature
$\Delta \dot{V}_{ca}$ = condenser air volume flow residual
$\Delta \dot{V}_{ea}$ = evaporator air volume flow residual
EvapFoul = evaporator fouling
FDD = fault detection and diagnosis
J = Jacobi matrix
k_{sc} = slope of refrigerant charge vs. liquid-line subcooling
k_{sh} = slope of refrigerant charge vs. suction line superheat
χ_{ref} = refrigerant quality
$\chi^2(n)$ = chi-square distribution
$(\chi^2)^{-1}\{,\}$ = inverse of the chi-square cumulative distribution function
LLRestr = liquid-line restriction
Λ = transformed diagonal matrix
M_{normal} = mean vector of normal operation residuals
$\dot{m}_{ref}$ = refrigerant mass flow rate
ω_i = fault class i
P = transform matrix
P_{dis} = discharge pressure
P_{ll} = liquid-line pressure
P_{sat} = saturated pressure
P_{suc} = suction pressure
P_x = Expansion device upstream refrigerant temperature
ϕ_{aie} = evaporator inlet air relative humidity
RefLeak = refrigerant leakage
RefLow = refrigerant low charge
RefHigh = refrigerant high charge
sign_stat( ) = signum operation function
$\sigma_{i,normal}$ = normal operation standard deviation for variable i
Σ_{normal} = covariance matrix for normal operation residuals
T_{aic} = condenser inlet air temperature
T_{aie} = evaporator inlet air temperature
T_{cond} = condensing temperature
T_{dis} = discharge line temperature
T_{evap} = evaporating temperature

T_{sh}	=	superheat	X	=	fault vector
T_{sc}	=	subcooling	Y	=	residual vector
T_{suc}	=	suction line temperature	Z	=	transformed feature vector
T_x	=	expansion device upstream refrigerant pressure			

REFERENCES

Breuker, M.S. 1997. Evaluation of a statistical, rule-based detection an diagnosis method for vapor compression air conditioners. Master's thesis, School of Mechanical Engineering, Purdue University, West Lafayette, IN.

Breuker, M.S., and J.E. Braun. 1998. Evaluating the performance of a fault detection and diagnostic system for vapor compression equipment. *HVAC&R Research* 4(4):401–23.

Comstock, M.C., J.E. Braun, and B. Chen. 1999. Literature review for application of fault detection and diagnostic methods to vapor compression cooling equipment, Ray W. Herrick Laboratories, Report # HL99-19. Purdue University, West Lafayette, IN.

Dexter, A.L., and D. Ngo. 2001. Fault diagnosis in air-conditioning systems: A multi-step fuzzy model-based approach. *HVAC&R Research* 7(1):83–102.

Dexter, A., and J. Pakanen, eds. 2001. Demonstrating automated fault detection and diagnosis methods in real buildings. *VTT Building Technology 2001, VTT Symposium 217, Espoo, Finland.*

Fukunaga, K. 1990. *Introduction to Statistical Pattern Recognition*. West Lafayette, IN: Academic Press.

Gerasenko, S. 2002. A web-based FDD for HVAC systems. Master's thesis, Computer Science, Cincinnati University, Cincinnati, Ohio.

Li, H. 2004. A decoupling-based unified fault detection and diagnosis approach for packaged air conditioners. PhD thesis, School of Mechanical Engineering, Purdue University, West Lafayette, IN.

Li, H., and J.E. Braun. 2003. An improved method for fault detection and diagnosis applied to packaged air conditioners. *ASHRAE Transactions* 109(2):683–92.

Li, H., and J.E. Braun. 2006. Decoupling features and virtual sensors for diagnosis of faults in vapor compression air conditioners. Accepted by *International Journal of Refrigeration*. In press.

Merriam-Webster. 2006. *Merriam-Webster Online*. http://m-w.com/dictionary/taxonomy.

Reddy, T.A., K.K. Andersen, and D. Niebur. 2003. Information content of incoming data during field monitoring: Application to online chiller modeling. *HVAC&R Research* l9(4):365–84.

Riemer, P.L., J.W. Michell, and W.A. Beckman. 2002. The use of time series analysis in fault detection and diagnosis methodologies. *ASHRAE Transactions* 108(2):384–94.

Rossi, T.M., and J.E. Braun. 1997. A statistical, rule-based fault detection and diagnostic method for vapor compression air conditioners. *HVAC&R Research* 3(1):19–37.

Shaw, S.R., L.K. Norford, D. Luo, and S.B. Leeb. 2002. Detection and diagnosis of HVAC faults via electrical load monitoring. *HVAC&R Research* 8(1):13–40.

Siegel, J.A., and C.P. Wray. 2002. An evaluation of superheat-based refrigerant charge diagnostics for residential cooling systems. *ASHRAE Transactions* 108(2):965–75.

Stallard, L.A. 1989. Model based expert system for failure detection and identification of household refrigerators. Master's thesis, School of Mechanical Engineering, Purdue University, West Lafayette, IN.

Yoshida, H., and S. Kumar. 2001a. Development of ARX model based off-line FDD technique for energy efficient buildings. *Energy Conversion & Management* 22:33–39.

Yoshida, H., and S. Kumar. 2001b. Online fault detection and diagnosis in VAV air handling unit by RARX modeling. *Energy Conversion & Management* 33:391–401.